American Mineralogist, Volume 90, pages 481–487, 2005

Mn-bearing "oxy-rossmanite" with tetrahedrally coordinated Al and B from Austria: Structure, chemistry, and infrared and optical spectroscopic study

ANDREAS ERTL,[1,*] GEORGE R. ROSSMAN,[2] JOHN M. HUGHES,[3] STEFAN PROWATKE,[4] AND THOMAS LUDWIG[4]

[1]Institut für Mineralogie und Kristallographie, Geozentrum, Universität Wien, Althanstrasse 14, 1090 Vienna, Austria
[2]Division of Geological and Planetary Sciences, California Institute of Technology, Pasadena, California 91125-2500, U.S.A.
[3]Department of Geology, Miami University, Oxford, Ohio 45056, U.S.A.
[4]Mineralogisches Institut, Universität Heidelberg, Im Neuenheimer Feld 236, 69120 Heidelberg, Germany

ABSTRACT

Pink, Mn-bearing "oxy-rossmanite" from a pegmatite in a quarry near Eibenstein an der Thaya, Lower Austria, has been characterized by crystal structure determination, chemical analyses (EMPA, SIMS), and optical absorption and infrared spectroscopy. Crystal structure refinements in combination with the chemical analyses give the optimized formulae $^{X}(\square_{0.53}Na_{0.46}Ca_{0.01})\ ^{Y}(Al_{2.37}Li_{0.33}Mn^{2+}_{0.25}Fe^{2+}_{0.04}Ti^{4+}_{0.01})\ ^{Z}Al_6\ ^{T}(Si_{5.47}Al_{0.28}B_{0.25})O_{18}(BO_3)_3\ ^{V}[(OH)_{2.85}O_{0.15}]\ ^{W}[O_{0.86}(OH)_{0.10}F_{0.04}]$, with $a = 15.8031(3)$, $c = 7.0877(3)$ Å, and $R = 0.017$ for the sample with 2.05 wt% MnO, and $^{X}(\square_{0.53}Na_{0.46}Ca_{0.01})\ ^{Y}(Al_{2.35}Li_{0.32}Mn^{2+}_{0.28}Fe^{2+}_{0.04}Ti^{4+}_{0.01})\ ^{Z}Al_6\ ^{T}(Si_{5.51}Al_{0.25}B_{0.24})O_{18}(BO_3)_3\ ^{V}[(OH)_{2.80}O_{0.20}]\ ^{W}[O_{0.86}(OH)_{0.10}F_{0.04}]$ for a sample with $a = 15.8171(3)$, $c = 7.0935(2)$ Å, $R = 0.017$, and 2.19 wt% MnO. Although the structure refinements show significant amounts of $^{[4]}$B, the <T-O> bond-lengths (~1.620 Å) mask the incorporation of $^{[4]}$B because of the incorporation of $^{[4]}$Al. The <T-O> distances, calculated using the optimized T site occupancies, are consistent with the measured distances. This "oxy-rossmanite" shows that it is possible to have significant amounts of $^{[4]}$B and $^{[4]}$Al in an Al-rich tourmaline. The "oxy-rossmanite" from Eibenstein has the highest known Al content of all natural tourmalines (~47 wt% Al_2O_3; ~ 8.6 apfu Al). The near-infrared spectrum confirms both that hydroxyl groups are present in the Eibenstein tourmaline and that they are present at a lower concentration than commonly found in other lithian tourmalines. The integrated intensity (850 cm^{-2}) of the OH bands in the single-crystal spectrum of "oxy-rossmanite" from Eibenstein is distinctly lower than for other Li-bearing tourmaline samples (970–1260 cm^{-2}) with OH contents >3.0 pfu. These samples fall on the V site = 3 (OH) line in the figure defining covariance of the relationship between the bond-angle distortion (σ_{oct}^2) of the ZO_6 octahedron and the <Y-O> distance. On a bond-angle distortion-<Y-O> distance diagram "oxy-rossmanite" from Eibenstein lies between the tourmalines that contain 3 (OH) at the V site, and natural buergerite, which contains 0.3 (OH) and 2.7 O at the V site. No H could be found at the O1 site by refinement, and the spherical electron density in the difference-Fourier map around the O1 site supports the conclusion that this site is mainly occupied by O. The pink color comes from the band at 555 nm that is associated with Mn^{3+} produced by natural irradiation of Mn^{2+}. This is the first time a tourmaline is described that has a composition that falls in the field of the previously proposed hypothetical species "oxy-rossmanite".

INTRODUCTION AND PREVIOUS WORK

Rossmanite, with the ideal end-member formula $\square(LiAl_2)Al_6(Si_6O_{18})(BO_3)_3(OH)_4$, is an alkali-deficient tourmaline described as a new tourmaline species from Rožná, western Moravia, Czech Republic, by Selway et al. (1998). The lattice parameters were given as $a = 15.770(2)$, $c = 7.085(1)$ Å. Its actual formula unit is $^{X}(\square_{0.57}Na_{0.43})^{Y}(Li_{0.71}Al_{2.17})^{Z}Al_6^{T}(Si_6O_{18})(B_{2.92}O_9)(OH)_{3.83}F_{0.10}O_{0.07}$ (Selway et al. 1998). This species was subsequently identified in additional pegmatite localities worldwide (Pezzotta and Guastoni 1998; Pezzotta et al. 1998; Selway et al. 1999, 2000, 2002; Wise 2000; Giller 2003; Korbel and Novák 2003; Pezzotta and Jobin 2003).

In their evaluation of tourmaline nomenclature, Hawthorne and Henry (1999) proposed "fluor-rossmanite", with the formula $\square(LiAl_2)Al_6(Si_6O_{18})(BO_3)_3(OH)_3F$, as a hypothetical tourmaline end-member. Subsequently, Giller (2003) reported an analysis of a pale pink tourmaline sample from Omapyo, Namibia, and also some compositions in faceted gemstones from Ibadan, Nigeria, which indicated "fluor-rossmanite". Hawthorne and Henry (1999) also proposed "oxy-rossmanite", with the formula $\square(Li_{0.5}Al_{2.5})Al_6(Si_6O_{18})(BO_3)_3(OH)_3O$, as a hypothetical tourmaline end-member. "Oxy-rossmanite" is characterized by a vacancy-dominated X site, an Al-dominated Y site (with a minor component of Li), and an O-dominated W site. We know of no previously described tourmaline that has been assigned to "oxy-rossmanite."

Ertl (1995) determined lattice parameters and qualitative chemical analyses of different tourmaline samples from a Moldanubian pegmatite, near the village of Eibenstein an der Thaya, Lower Austria (geologic unit "Bunte Serie"). The

* E-mail: andreas.ertl@a1.net

mineral constituents of this granitic pegmatite include olenite, schorl, dravite, quartz, muscovite, beryl, and apatite (Ertl 1995). Red to pale-blue, Al-rich tourmaline with lattice parameters a = 15.802–15.869 and c = 7.086–7.103 Å was originally assigned to olenite and elbaite by Ertl (1995) in the absence of quantitative major element analyses including light elements. In this article, we provide detailed analyses of the reddish Al-rich tourmaline from that pegmatite, with structural, chemical, and spectroscopic data that indicate that it corresponds to the previously theoretical "oxy-rossmanite" composition (Hawthorne and Henry 1999).

Experimental details

Sample selection

A single pink tourmaline crystal (~5 mm in diameter, ~2 cm in length) was found in a pegmatite in a quarry ~800 m northeast of the village of Eibenstein an der Thaya in Lower Austria. Portions of this crystal were deposited as sample NMNH 173824 at the National Museum of Natural History, Smithsonian Institution, Washington DC, and as sample 134790 at the Mineralogical Museum, Harvard University, Cambridge, Massachusetts. Note that this locality is different from that of the Mn-rich tourmaline from Eibenstein an der Thaya described by Ertl et al. (2003b, 2004). The pink crystal has a 0.017 mm thick greenish outer zone of Fe-bearing olenite. A preliminary crystal structure determination of a pink fragment of this tourmaline crystal showed relatively short lattice parameters compared to elbaite and a refined occupancy of Na < 50% at the X site. The structures of four pink fragments were refined using the methods described below. The two samples (each is ~100 μm in diameter) with the shortest (REDT1) and longest (REDT4) lattice parameters are described in this study.

Crystal structure

The tourmaline crystals were mounted on a Bruker Apex CCD diffractometer equipped with graphite-monochromated Mo$K\alpha$ radiation. Refined cell-parameters and other crystal data are listed in Table 1. Redundant data were collected for an approximate sphere of reciprocal space, and were integrated and corrected for Lorentz and polarization factors using the Bruker program SAINTPLUS (Bruker AXS Inc. 2001).

The structure was refined using the tourmaline starting model and the Bruker SHELXTL V. 6.10 package of programs, with neutral-atom scattering factors and terms for anomalous dispersion. Refinement was performed with anisotropic thermal parameters for all non-hydrogen atoms. In Table 2 we list the atom parameters, and in Table 3 we present selected interatomic distances.

Table 1. Crystal data and results of structure refinement for Mn-bearing "oxy-rossmanite" from Eibenstein an der Thaya, Lower Austria

Space group:	*R*3*m*
Unit-cell parameters (Å):	
REDT1:	a = 15.8031(3), c = 7.0877(3)
REDT4:	a = 15.8171(3), c = 7.0935(2)
Frame width	0.20°
Scan time	15 s
Number of frames	4500,
Detector distance	5 cm
Measured reflections, full sphere:	
REDT1:	35,757
REDT4:	35,747
Unique reflections; refined parameters:	
REDT1:	1340, 93
REDT4:	1096, 94
$R1$, $I > 4\sigma_I$:	
REDT1:	0.0165
REDT4:	0.0167
Difference peaks (+,–):	
REDT1:	0.31, 0.25
REDT4:	0.30, 0.27
Goodness-of-Fit:	
REDT1:	1.203
REDT4:	1.221

Chemical analyses

The two crystals selected for crystal structure determination were prepared as a polished section for chemical analysis. All elements except B, Li, Be, and H were determined with a Cameca SX51 electron microprobe (EMP) equipped with five wavelength-dispersive spectrometers (Universität Heidelberg). Operating conditions were as follows: 15 kV accelerating voltage, 20 nA beam current, and beam diameter 5 μm. Peaks for all elements were measured for 10 s, except for Mg (20 s), Cr (20 s), Ti (20 s), Zn (30 s), and F (40 s). Natural and synthetic silicate and oxide standards were used for calibration (Ertl et al. 2003b). The analytical data were reduced and corrected using the PAP routine. A modified matrix correction was applied assuming stoichiometric O atoms and all non-measured components as B_2O_3. The accuracy of the electron-microprobe analyses and the correction procedure was checked by measuring three samples of reference tourmalines (98114: elbaite, 108796: dravite, 112566: schorl). Compositions of these tourmaline samples are presented in the context of an interlaboratory comparison study (Dyar et al. 1998, 2001). Coincidence between the published analyses and the measured values was satisfactory. Under the described conditions, analytical errors for all analyses are ± 1% relative for major elements and ±5% relative for minor elements.

H, Be, Li, and B were determined by secondary ion mass spectrometry (SIMS) with a CAMECA ims 3f ion microprobe. Primary O-ions were accelerated to 10 keV. The mass spectrometer's energy window was set to 40 eV. An offset of 75 V was applied to the secondary accelerating voltage of 4.5 kV so that secondary ions with an initial energy of 75(20) eV were analyzed (energy filtering). This adjustment suppresses effects of light elements related to the matrix (Ottolini et al. 1993). For B, Be, and Li the primary current was 20 nA, resulting in a sputtering surface of ~30 μm in diameter. The spectrometer's mass resolution, $M/\Delta M$, for B, Be, and Li was set to ~1100 (10%) to suppress interferences ($^6LiH^+$, $^{10}BH^+$, Al^{3+}). Secondary ions ^7Li, ^9Be, and ^{11}B were collected under an ion-imaged field of 150 μm diameter.

For H, the primary beam current was 20 nA and $M/\Delta M$ was set to ~400 (10%). To reduce the rate of contamination with water, a smaller field aperture was chosen; thus, the analyzed area was restricted to 10 μm in diameter in the center of the scanned area. This method reduces the effect of water contamination, which was found to be higher on the edge of the primary beam spot than in the center. Water contamination was further reduced by using a liquid nitrogen cold-trap attached to the sample chamber of the instrument. The count rates of the analyzed isotopes (^1H, ^7Li, ^9Be, and ^{11}B) were normalized to the count rate of ^{30}Si.

The relative ion yield (RIY) for B was determined using three different tourma-

Table 2. Table of atom parameters in Mn-bearing "oxy-rossmanite" from Eibenstein an der Thaya, Lower Austria

Atom	*x*	*y*	*z*	U_{eq}	Occ.
RED T1:					
Na	0.0000	0.0000	0.2500	0.0275(12)	$Na_{0.484(2)}$
Si	0.19154(2)	0.18958(2)	0.0303(5)	0.00598(10)	$Si_{0.946(4)}B_{0.054}$
B	0.10956(7)	0.21912(14)	0.4803(6)	0.0077(3)	$B_{1.00}$
AlY	0.12146(4)	0.06073(2)	–0.3362(5)	0.00814(16)	$Al_{0.994(4)}$
AlZ	0.29651(3)	0.25999(3)	–0.3643(5)	0.00762(9)	$Al_{1.00}$
O1	0.0000	0.0000	–0.2052(6)	0.0149(4)	$O_{1.00}$
O2	0.06065(5)	0.12131(10)	0.5205(5)	0.0130(3)	$O_{1.00}$
O3	0.25787(11)	0.12893(6)	–0.4636(5)	0.0126(3)	$O_{1.00}$
O4	0.09524(5)	0.19049(11)	0.1043(5)	0.0124(2)	$O_{1.00}$
O5	0.18806(11)	0.09403(5)	0.1258(5)	0.0127(2)	$O_{1.00}$
O6	0.19340(6)	0.18302(7)	–0.1974(5)	0.00945(16)	$O_{1.00}$
O7	0.28717(7)	0.28662(6)	0.1044(5)	0.00906(16)	$O_{1.00}$
O8	0.20959(7)	0.27052(7)	0.4649(5)	0.00910(16)	$O_{1.00}$
H3	0.251(3)	0.1256(15)	0.423(6)	0.053(13)	$H_{1.00}$
REDT4:					
Na	0.0000	0.0000	0.2500	0.0278(14)	$Na_{0.478(1)}$
Si	0.19152(3)	0.18960(3)	0.0302(6)	0.00585(14)	$Si_{0.935(4)}B_{0.065}$
B	0.10969(9)	0.21937(18)	0.4801(7)	0.0084(4)	$B_{1.00}$
AlY	0.12150(5)	0.06075(2)	–0.3364(6)	0.0087(2)	$Al_{1.000(4)}$
AlZ	0.29652(3)	0.26001(3)	–0.3646(6)	0.00795(12)	$Al_{1.00}$
O1	0.0000	0.0000	–0.2049(7)	0.0148(5)	$O_{1.00}$
O2	0.06064(6)	0.12128(12)	0.5202(7)	0.0134(3)	$O_{1.00}$
O3	0.25794(13)	0.12897(7)	–0.4638(6)	0.0128(3)	$O_{1.00}$
O4	0.09530(7)	0.19060(13)	0.1038(6)	0.0133(3)	$O_{1.00}$
O5	0.18804(13)	0.09402(7)	0.1252(6)	0.0138(3)	$O_{1.00}$
O6	0.19336(8)	0.18311(8)	–0.1976(6)	0.0101(2)	$O_{1.00}$
O7	0.28715(8)	0.28675(7)	0.1038(6)	0.0093(2)	$O_{1.00}$
O8	0.20954(8)	0.27049(8)	0.4646(6)	0.0098(2)	$O_{1.00}$
H3	0.246(3)	0.1231(17)	0.415(7)	0.054(14)	$H_{1.00}$

TABLE 3. Selected interatomic distances in Mn-bearing "oxy-rossmanite" from Eibenstein an der Thaya, Lower Austria

	REDT1	REDT4
X-		
O2 ×3	2.536(3)	2.537(4)
O5 ×3	2.720(2)	2.724(2)
O4 ×3	2.804(2)	2.809(2)
Mean	2.687	2.690
Y-		
O1	1.904(1)	1.908(2)
O2 ×2	1.947(1)	1.949(1)
O6 ×2	1.949(1)	1.951(1)
O3	2.074(2)	2.076(2)
Mean	1.962	1.964
Z-		
O7	1.8796(9)	1.881(1)
O8	1.881(1)	1.882(1)
O6	1.885(1)	1.887(1)
O8′	1.899(1)	1.902(1)
O7′	1.9323(9)	1.932(1)
O3	1.9730(7)	1.975(1)
Mean	1.908	1.910
T-		
O7	1.6105(9)	1.6118(11)
O6	1.6164(6)	1.6166(7)
O4	1.6183(10)	1.6202(13)
O5	1.6303(7)	1.6309(8)
Mean	1.6189	1.6199
B-		
O2	1.369(2)	1.372(2)
O8 (×2)	1.374(1)	1.373(3)
Mean	1.372	1.373

lines as reference material: elbaite (98144), dravite (108796), and schorl (112566), all described and analyzed by Dyar et al. (1998, 2001). The RIY for H was determined using elbaite (98144) as reference material, because this tourmaline sample also has a relatively high Al content. The reference material for Li and Be was the SRM610 standard glass by NIST with concentrations for Li and Be published by Perkins et al. (1997). The relative reproducibility (1σ) for the RIY of B, Li, and Be was <1%. Matrix effects and the uncertainty of the element concentrations in the reference material limit the accuracy of the analysis. The relative uncertainty is estimated to be <30% for H, <20% for Li, and <10% for B. Table 4 contains complete chemical analyses for this Al-rich tourmaline.

Optical spectra

A 380 × 185 µm crystal fragment of this tourmaline was prepared as a 92.8 µm thick parallel plate polished on both sides. Polarized optical absorption spectra in the 390–1100 nm range were obtained at about one nm resolution with a locally built microspectrometer system (California Institute of Technology, Pasadena) consisting of a 1024-element Si diode-array detector coupled to a grating spectrometer system via fiber optics to a highly modified NicPlan infrared microscope containing a calcite polarizer. A pair of conventional 10× objectives was used as an objective and a condenser. Spectra were obtained through the central area of the sample which included a veil of two phase (liquid/gas) inclusions.

Infrared spectra

Infrared spectra were obtained in the main compartment of a Nicolet Magna 860 FTIR spectrometer at 2 cm^{-1} resolution using a 200 µm aperture. Near-IR spectra were obtained using a CaF_2 beamsplitter, tungsten-halogen source, MCT-A detector, and a $LiIO_3$ polarizer and were averaged over 256 to 4000 scans. For the smallest crystals, a silica beamsplitter and InSb detector were used to collect the spectra. Additional spectra were obtained with a Nicolet Continµum infrared microscope using a MCT-A/CaF_2/tungsten-halogen combination.

Total integrated band area ($Area_{tot} = Area_{Elle} + 2 \times Area_{E\perp c}$) was determined for the mid-IR OH overtone bands using the Omnic E.S.P. 5.2 software of the FTIR spectrometer. Before integration, a minor, visually estimated, background correction was needed to correct for a sloping background. Integrated absorbances were determined by establishing a suitable linear baseline under the OH region and measuring the area between the curve and the baseline over the region of the OH bands. The baseline was connected to the spectral trace on both the high- and low-energy side of the OH region. This was done with a spectrum normalized for a 1 cm thick crystal.

TABLE 4. Composition of Mn-bearing "oxy-rossmanite" from Eibenstein an der Thaya, Lower Austria (wt%)

	REDT1[1,2]	REDT1[3]	REDT4[1,2]	REDT4[3]
SiO_2	33.96	34.56	34.04	34.78
TiO_2	0.10	0.08	0.11	0.08
B_2O_3	11.77	11.90	11.64	11.85
Al_2O_3	47.08	46.37	47.04	46.05
FeO*	0.29	0.30	0.31	0.30
MnO*	2.05	1.87	2.19	2.09
MgO	0.01	–	0.01	–
CaO	0.04	0.06	0.04	0.06
Li_2O	0.25	0.52	0.24	0.50
ZnO	0.03	–	0.01	–
Na_2O	1.51	1.50	1.51	1.50
K_2O	0.01	–	0.01	–
F	0.09	0.08	0.09	0.08
H_2O	3.07	2.79	2.90	2.74
O≡F	–0.04	–0.03	–0.04	–0.03
Sum	100.22	100.00	100.10	100.00
N	31	31	31	31
Si	5.37	5.47	5.40	5.51
$^{[4]}$Al	0.42	0.28	0.41	0.25
$^{[4]}$B	0.21	0.25	0.19	0.24
Sum T site	6.00	6.00	6.00	6.00
$^{[3]}$B	3.00	3.00	3.00	3.00
Al	8.35	8.37	8.38	8.35
Mn^{2+}	0.27	0.25	0.29	0.28
Fe^{2+}	0.04	0.04	0.04	0.04
Mg	0.00	–	0.00	–
Zn	0.00	–	0.00	–
Ti^{4+}	0.01	0.01	0.01	0.01
Li	0.16	0.33	0.15	0.32
Sum Y, Z sites	8.83	9.00	8.87	9.00
Ca	0.01	0.01	0.01	0.01
Na	0.46	0.46	0.46	0.46
K	0.00	–	0.00	–
□	0.53	0.53	0.53	0.53
Sum X site	1.00	1.00	1.00	1.00
Sum cations	18.30	18.47	18.34	18.47
OH	3.24	2.95	3.07	2.90
F	0.04	0.04	0.04	0.04
Sum OH + F	3.28	3.00	3.11	2.94

Notes: [1] Average of 25 EMP analyses. [2] Average of 2 SIMS analyses for B_2O_3, Li_2O, and BeO and 1 SIMS analyses for H_2O. For sample REDT1 BeO = 9 ppm, and for sample REDT4 BeO = 10 ppm. [3] Weight percent calculated from optimal site occupancies and normalized to 100%.
* Total Mn and total Fe calculated as MnO (see text) and FeO. Cl and Cr are below the detection limit in both samples.

RESULTS AND DISCUSSION

Structure

Using quadratic programming methods, Wright et al. (2000) offered a method of optimizing the occupants of cation sites in minerals with multiply occupied cation sites; the optimized formula essentially minimizes the differences between the formula obtained from the results of the chemical analysis and that obtained by single crystal structure refinement (SREF). Using that method with the structure refinement and chemical data obtained in this study, the structural formulae of these tourmaline samples are:

REDT1: $^{X}(\square_{0.53}Na_{0.46}Ca_{0.01})\,^{Y}(Al_{2.37}Li_{0.33}Mn^{2+}_{0.25}Fe^{2+}_{0.04}Ti^{4+}_{0.01})\,^{Z}Al_6\,^{T}(Si_{5.47}Al_{0.28}B_{0.25})O_{18}(BO_3)_3\,^{V}[(OH)_{2.85}O_{0.15}]\,^{W}[O_{0.86}(OH)_{0.10}F_{0.04}]$

REDT4: $^{X}(\square_{0.53}Na_{0.46}Ca_{0.01})\,^{Y}(Al_{2.35}Li_{0.32}Mn^{2+}_{0.28}Fe^{2+}_{0.04}Ti^{4+}_{0.01})\,^{Z}Al_6\,^{T}(Si_{5.51}Al_{0.25}B_{0.24})O_{18}(BO_3)_3\,^{V}[(OH)_{2.80}O_{0.20}]\,^{W}[O_{0.86}(OH)_{0.10}F_{0.04}]$

No H could be found at the O1 site by refinement, and the difference-Fourier map around the O1 site showed no peak associated with H. The map shows a spherical electron density similar to that described by Cámara et al. (2002) [Fig. 1a of that paper, crystal 1, dravite, with 0.18 (OH) at the O1 site (W site)]. Dyar et al. (2001) gave for the same tourmaline sample (dravite, 108796) an occupancy of ($O_{0.80}F_{0.20}$), but no (OH) at the O1 site. Therefore we chose an average value for ^{W}(OH), given in Dyar et al. (2001) and Cámara et al. (2002) for the O1 site of this tourmaline sample. Ertl et al. (2002) showed that the bond-angle distortion (σ_{oct}^2) of the ZO_6 octahedron in a tourmaline is largely a function of the <Y-O> distance, although the occupant of the O3 site (V site) also affects that distortion. The covariance, *r*, of <Y-O> and the σ_{oct}^2 of the ZO_6 octahedron is –0.991 (Fig. 1) for all investigated tourmalines that have 3 (OH) groups, including the samples from Hughes et al. (2004). In Figure 1, this tourmaline lies between those that contain 3 (OH) at the V site and natural buergerite, which contains 0.3 (OH) and 2.7 O at the V site (Dyar et al. 1998). The total (OH) content in the optimized formulae (Table 4) was calculated to produce charge-balanced formulae. The recalculated wt% for H_2O is 6–9% lower than the measured values (by SIMS). One possible explanation for the higher values as obtained by SIMS is that this tourmaline from Eibenstein contains significant fluid inclusions that contain H_2O (Fig. 2). However, these errors are still lower than the relative uncertainty of the SIMS analyses.

Although the structure refinements show significant amounts of $^{[4]}$B (0.32–0.39 apfu; Table 2), the <T-O> bond-lengths are in the range 1.619–1.620 Å (Table 3), which is similar to a T site fully occupied with Si (MacDonald and Hawthorne 1995; Bloodaxe et al. 1999). There appears to be $^{[4]}$B on the basis of the chemical analyses, although the excess B (>3.00 apfu) is within the 10% relative uncertainty associated with the SIMS analysis of B. However, the structure refinements (while fixing the Z site at $Al_{1.00}$; Table 2), are in accord with the presence of $^{[4]}$B. Tourmaline samples with no $^{[4]}$B (and no significant amounts of $^{[4]}$Al) give higher refined Si values (>5.80 apfu), while fixing the Z site at full occupancy by Al. Because of a relatively low Si content in both samples (~5.4 apfu Si; Table 4), these bond lengths can be explained by significant amounts of $^{[4]}$Al in addition to $^{[4]}$B. The <T-O> distances, calculated with formula (1) in Ertl et al. (2001), using the optimized T-site occupants, are consistent with the measured distances ($<T\text{-}O>_{calc.}$ = 1.620 Å for both samples). This sample shows that it is possible to have significant amounts of $^{[4]}$B and $^{[4]}$Al in an Al-rich tourmaline. This tourmaline from Eibenstein has the highest known Al content of all natural tourmalines (up to 47.08 wt% Al_2O_3; up to ~8.64 apfu Al). Very high Al contents were also found in colorless (B-rich) olenite from Koralpe, Styria, Austria (up to 46.53–46.71 wt% Al_2O_3 and 8.46 apfu Al; Ertl et al. 1997; Hughes et al. 2000), and in olenite from the type locality, Olenii Range, Voron'i Tundry, Kola Peninsula, Russia (up to 45.79–46.43 wt% Al_2O_3 and 8.52 apfu Al; Sokolov et al. 1986; Schreyer et al. 2002). Structural refinements of the X site of both samples confirm Na occupancy of <50% [Table 2; only very small amounts of Ca (0.04 wt% CaO) and K (0.01 wt% K_2O) were found by chemical analyses (Table 4)].

The chemical and structural data for this sample are consistent with the hypothetical species "oxy-rossmanite", $\square(Li_{0.5}Al_{2.5})Al_6(Si_6O_{18})(BO_3)_3(OH)_3O$, described by Hawthorne and Henry (1999). The X site contains more than 50% vacancies, which it puts it in the X-site deficient rossmanite-foititemagnesiofoitite group. The Y site contains mainly Al and some Li, which constrains the sample to the rossmanite group, and the W site is dominated by O^{2-}, indicating the hypothetical species "oxy-rossmanite". However, like rossmanite from the type locality (Selway et al. 1998), "oxy-rossmanite" from Eibenstein shows a significant amount of Na at the X site (Table 4) and minor amounts of other components.

Because there is no evidence for vacancies at the Y site in "oxy-rossmanite" from Eibenstein, the Li content for the optimized formulae was calculated by assuming there are no vacancies at the Y site. The recalculated Li_2O content for the optimized formulae is higher than the values, measured by SIMS. The unusually high Al content of this tourmaline, resulting in a

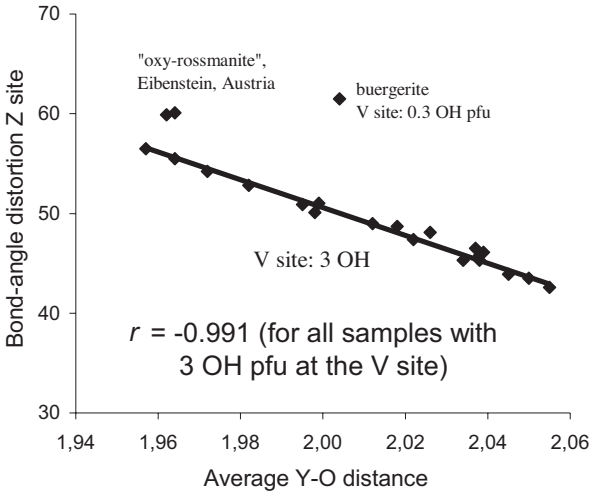

FIGURE 1. Relationship between bond-angle distortion (σ_{oct}^2) of the ZO_6 octahedron and the average Y-O distance. Modified from Figure 3 from Ertl et al. (2002), including the structural data from Hughes et al. (2004).

FIGURE 2. Inclusions in "oxy-rossmanite" from Eibenstein an der Thaya, Lower Austria (polished section: 65 × 90 μm).

relatively high matrix effect, could be an explanation. However, the electrons of the final assigned occupants at the Y sites are in a good agreement with the structure refinements (Table 2). The relatively low Li content for such an Al-rich natural tourmaline is in good agreement with the low F and Na contents observed in the typical positive correlation between these elements in tourmaline because of the geochemical growth environment.

Optical spectroscopy

The optical absorption spectrum of "oxy-rossmanite" (Fig. 3) is more intense in the **E**⊥**c** direction. It consists of a band at about 555 nm and weaker features near 450 and 415 nm. The **E**‖**c** spectrum also contains the 555 nm band that overlaps another broad band near 475 nm. There is also an indication of a weak band near 780 nm. The broad rise in absorption from long- to low-energy could be due in part to scattering from imperfections in the crystal and partly to an ultraviolet absorption band. The spectrum is broadly similar to the spectrum of rossmanite (Fig. 4), but the major bands are shifted to longer wavelengths. For example, in rossmanite, the main band is at 517 nm.

The pink color of "oxy-rossmanite" comes from the band at 555 nm that is associated with Mn^{3+} produced by natural irradiation of Mn^{2+}, as has been previously described for elbaite (Reinitz and Rossman 1988).

Infrared spectroscopy

The infrared spectrum obtained in the mid infrared region confirms both that hydroxyl groups are in the Eibenstein tourmaline, and that they are present at a lower concentration than commonly found in other lithian tourmalines. The spectrum (Fig. 5) shows OH bands in the **E**‖**c** spectrum at 7175, 7144, 7022, ~6964 cm^{-1}, and the most prominent band at 6708 cm^{-1}. These bands are shifted to lower wavenumbers than the corresponding bands in elbaite of similar divalent cation composition such as GRR 596-Afgh-1 (elbaite from Afghanistan) that has bands at 7180 (weak), 7133, 7001 (prominent), and 6778 cm^{-1} (Fig. 6).

Mattson (1985) concluded that the 7001 cm^{-1} band in GRR 598-Afgh-1 is associated with H bound to the O3 site with a local configuration involving Li^{+}. This band is of low intensity in "oxy-rossmanite" compared to the Afgh-1 standard elbaite. The low intensity of these OH bands suggests that the absolute OH concentration is lower than that in GRR 598-Afgh-1. There has not been an absolute calibration of the intensity of the OH overtone bands in the tourmaline spectrum, so it is not possible at this time to establish an absolute concentration. Nevertheless, it is worth comparing the OH intensity of "oxy-rossmanite" to other relevant tourmalines.

The integrated intensity of OH bands (normalized to 1 cm thickness) in the single crystal spectra of the Eibenstein

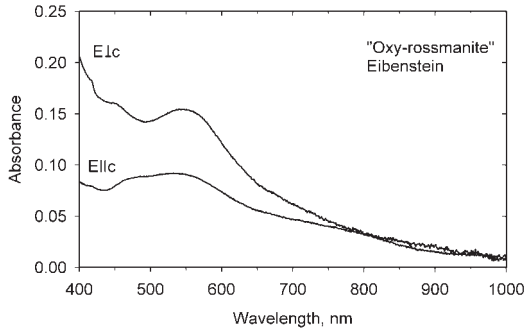

FIGURE 3. Optical absorption spectrum of a 0.0928 mm thick crystal of Mn-bearing "oxy-rossmanite".

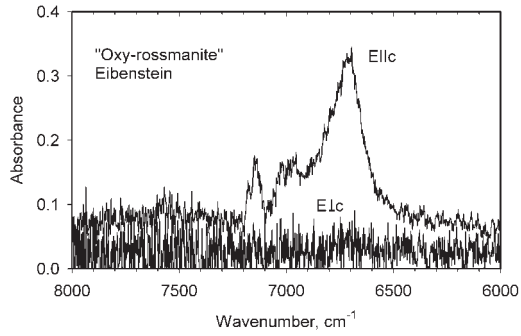

FIGURE 5. Near infrared spectrum of "oxy-rossmanite" from Eibenstein in the OH overtone region. A 0.0928 mm thick crystal plotted normalized to 1.0 mm thickness.

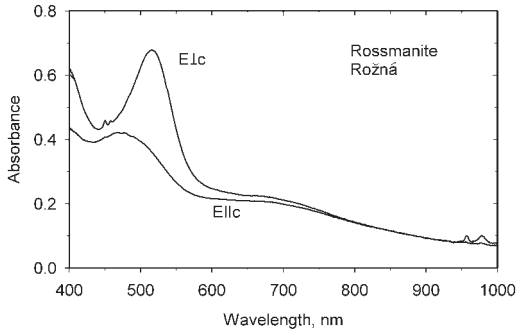

FIGURE 4. Optical absorption spectrum of a 2.976 mm thick crystal of rossmanite plotted normalized to 3.0 mm thickness.

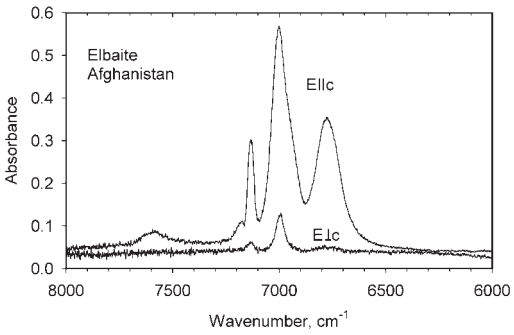

FIGURE 6. Near infrared spectrum of elbaite GRR 598-Afgh-1 from Afghanistan in the OH overtone region. Thickness: 0.567 mm.

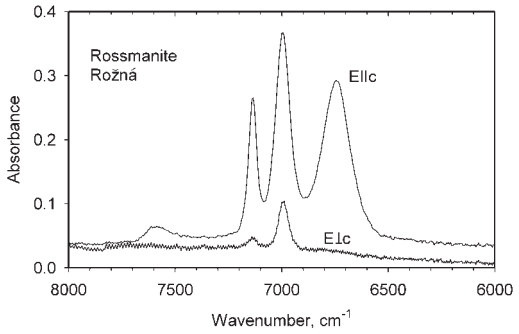

FIGURE 7. Near infrared spectrum of rossmanite from the Rožná in the OH overtone region. A 2.967 mm thick crystal plotted normalized to 1.0 mm thickness.

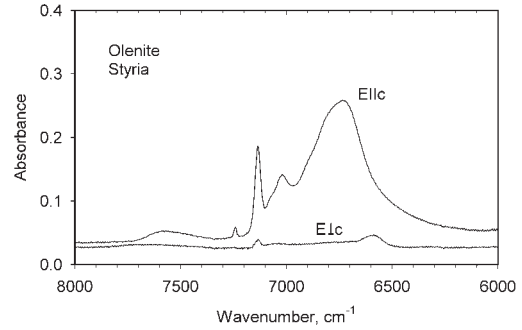

FIGURE 8. Near infrared spectrum of boron-rich olenite from Koralpe, Styria, Austria. A 0.278 mm thick crystal plotted normalized to1.0 mm thickness.

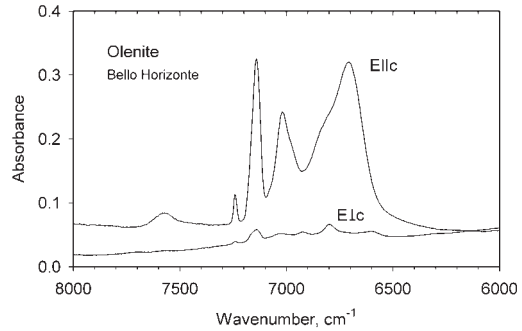

FIGURE 9. Near infrared spectrum of olenite GRR 1796a, from the Bello Horizonte Mine, California, in the OH overtone region. A 1.933 mm thick crystal plotted normalized to 1.0 mm thickness.

"oxy-rossmanite" is 850 cm^{-2}, whereas it is 1260 cm^{-2} for elbaite GRR 598-Afgh-1. Other comparisons of OH integrated intensities also point to a lower OH intensity in the Eibenstein "oxy-rossmanite". The intensity for the bands in the spectra of other tourmaline specimens are 970 cm^{-2} for rossmanite from Rožná, Czech Republic (Fig. 7); 1030 cm^{-2} for colorless olenite from Koralpe, Styria, Austria (Fig. 8), which contains ~3.3–3.4 OH (Ertl et al. 1997; Hughes et al. 2000; Kalt et al. 2001); and 1100 cm^{-2} for colorless olenite from the Bello Horizonte Mine, Riverside County, California (Fig. 9). As an aside, we note that according to the ideal formula of Hawthorne and Henry (1999), olenite should have a low OH content. In practice, all published olenite formulae to date have much higher OH contents due to a variety of minor substitutions that require H^+ for charge compensation (e.g., Ertl et al. 1997, 2003a, 2003b; Hughes et al. 2000, 2004; Schreyer et al. 2002). Thus it is not surprising that the near-IR spectra of our olenite samples also have relatively high OH band intensities.

Of twenty-five elbaite, liddicoatite, and rossmanite samples examined to date (Rossman et al., in prep.) "oxy-rossmanite" remains the sample with an integrated intensity that is significantly lower than the others. All of these observations are highly suggestive that the "oxy-rossmanite" contains a lower amount of OH than most other tourmalines.

Why does this tourmaline sample have such a low OH content? Because it has a low Li content, higher oxidation state cations must occupy the Y site. In this case, Al is the dominant cation at the Y site. For a charge-balanced formula, other sites must have appropriate charges to accommodate the "excess" positive charge at the Y site. The choices are cation vacancies at the X site, trivalent cations at the tetrahedral site, and oxy-substitution at the OH sites. In fact, all three of these possibilities are observed in the Eibenstein tourmaline.

ACKNOWLEDGMENTS

We thank A. Prayer, Irnfritz, Lower Austria, for providing the tourmaline samples and A. Wagner, Vienna, Austria, for preparing them. This work was supported in part by NSF grants EAR-0003201 and EAR-9804768 to J.M.H., and EAR-0125767 and EAR-0337816 to G.R.R. We sincerely thank D. Henry and E.S. Grew for their careful reviews of the manuscript.

REFERENCES CITED

Bloodaxe, E.S., Hughes, J.M., Dyar, M.D., Grew, E.S., and Guidotti, C.V. (1999) Linking structure and chemistry in the Schorl-Dravite series. American Mineralogist, 84, 922–928.

Cámara, F., Ottolini, L., and Hawthorne, F.C. (2002) Chemistry of three tourmalines by SREF, EMPA, and SIMS. American Mineralogist, 87, 1437–1442.

Dyar, M.D., Taylor, M.E., Lutz, T.M., Francis, C.A., Guidotti, C.V., and Wise, M. (1998) Inclusive chemical characterization of tourmaline: Mössbauer study of Fe valence and site occupancy. American Mineralogist, 83, 848–864.

Dyar, M.D., Wiedenbeck, M., Robertson, D., Cross, LR., Delaney, J.S., Ferguson, K., Francis, C.A., Grew, E.S., Guidotti, C.V., Hervig, R.L., Hughes, J.M., Husler, J., Leeman, W., McGuire, A.V., Rhede, D., Rothe, H., Paul, R.L., Richards, I., and Yates, M. (2001) Reference minerals for the microanalysis of light elements. Geostandards Newsletter, 25, 441–463.

Ertl, A. (1995) Elbait, Olenit, Dravit-Buergerit-Mischkristalle, Dravit, Uvit und ein neuer Al-Turmalin (?) von österreichischen Fundstellen. Mitteilungen der Österreichischen Mineralogischen Gesellschaft, 140, 55–72.

Ertl, A., Pertlik, F., and Bernhardt, H.-J. (1997) Investigations on olenite with excess boron from the Koralpe, Styria, Austria. Österreichische Akademie der Wissenschaften, Mathematisch-Naturwissenschaftliche Klasse, Abt. I, Anzeiger, 134, 3–10.

Ertl, A., Hughes, J.M., and Marler, B. (2001) Empirical formulae for the calculation of <*T*-O> and *X*-O2 bond lengths in tourmaline and relations to tetrahedrally coordinated boron. Neues Jahrbuch Mineralogie Monatshefte, 12, 548–557.

Ertl, A., Hughes, J.M., Pertlik, F., Foit, F.F. Jr., Wright, S.E., Brandstätter, F., and Marler, B. (2002) Polyhedral distortions in tourmaline. Canadian Mineralogist, 40, 153–162.

Ertl, A., Hughes, J.M., Brandstätter, F., Dyar, M.D., and Prasad, P.S.R. (2003a) Disordered Mg-bearing olenite from a granitic pegmatite at Goslarn, Austria: a chemical, structural, and infrared spectroscopic study. Canadian Mineralogist, 41, 1363–1370.

Ertl, A., Hughes, J.M., Prowatke, S., Rossman, G.R., London, D., and Fritz, E.A. (2003b) Mn-rich tourmaline from Austria: structure, chemistry, optical spectra, and relations to synthetic solid solutions. American Mineralogist, 88, 1369–1376.

Ertl, A., Schuster, R., Prowatke, S., Brandstätter, F., Ludwig, T., Bernhardt, H.-J., Koller, F., and Hughes J.M. (2004) Mn-rich tourmaline and fluorapatite in a Variscan pegmatite from Eibenstein an der Thaya, Bohemian massif, Lower Austria. European Journal of Mineralogy, 16, 551–560.

Giller, B.S. (2003) An overview of tourmaline mineralogy from gem tourmaline

producing pegmatite districts in Africa. M.Sc. Thesis, University of New Orleans, Lousianna.
Hawthorne, F.C. and Henry, D.J. (1999) Classification of the minerals of the tourmaline group. European Journal of Mineralogy, 11, 201–215.
Hughes, J.M., Ertl, A., Dyar, M.D., Grew, E., Shearer, C.K., Yates, M.G., and Giudotti, C.V. (2000) Tetrahedrally coordinated boron in a tourmaline: Boron-rich olenite from Stoffhütte, Koralpe, Austria. Canadian Mineralogist, 38, 861–868.
Hughes, J.M., Ertl, A., Dyar, M.D., Grew, E., Wiedenbeck, M., and Brandstätter, F. (2004) Structural and chemical response to varying [4]B content in zoned Fe-bearing olenite from Koralpe, Austria. American Mineralogist, 89, 447–454.
Kalt, A., Schreyer, W., Ludwig, T., Prowatke, S., Bernhardt, H.-J., and Ertl, A. (2001) Complete solid solution between magnesian schorl and lithian excess-boron olenite in a pegmatite from Koralpe (eastern Alps, Austria). European Journal of Mineralogy, 13, 1191–1205.
Korbel, P. and Novák, M. (2003) The Complete Mineral Encyclopedia, pp. 230. Gramercy Books, N.Y.
MacDonald, D.J. and Hawthorne, F.C. (1995) The crystal chemistry of Si ⇔ Al substitution in tourmaline. Canadian Mineralogist, 33, 849–858.
Mattson, S.M. (1985) Optical Expressions of Ion-Pair Interactions in Minerals. Ph.D. Thesis, California Institute of Technology.
Ottolini, L., Bottazzi, P., and Vannucci, R. (1993) Quantification of lithium, beryllium, and boron in silicates by secondary Ion Mass Spectrometry using conventional energy filtering. Analytical Chemistry, 65, 1960–1968.
Perkins, W.T., Pearce, N.J.G., and Westgate, J.A. (1997) The development of laser ablation ICP-MS and calibration strategies; examples from the analyses of trace elements in volcanic glass shards and sulfide minerals. Geostandards Newsletter, 21, 115–144.
Pezzotta, F. and Guastoni, A. (1998) Rossmanit, ein neuer Tourmalin aus Rozná (CR) and Elba. Lapis, 1998/9, 38–40.
Pezzotta, F. and Jobin, M. (2003) The Anjahamiary pegmatite, Fort Dauphin area, Madagascar. Pegmatite Interest Group (PIG), Mineralogcal Society of America, http://www.minsocam.org/MSA/Special/Pig.
Pezzotta, F., Guastoni, A., and Aurisicchio, C. (1998) La rossmanite di Rozna e dell'Elba. Rivista Mineralogica Italiana, 22, 46–50.
Reinitz, I.L. and Rossman, G.R. (1988) Role of natural radiation in tourmaline coloration. American Mineralogist, 73, 822–825.
Schreyer, W., Hughes, J.M., Bernhardt, H.-J., Kalt, A., Prowatke, S., and Ertl, A. (2002) Reexamination of olenite from the type locality: detection of boron in tetrahedral coordination. European Journal of Mineralogy, 14, 935–942.
Selway, J.B., Novák, M., Hawthorne, F., Černý, P., Ottolini, L., and Kyser, T.K. (1998) Rossmanite, □(LiAl$_2$) Al$_6$ (Si$_6$O$_{18}$) (BO$_3$)$_3$ (OH)$_4$, a new alkali-deficient tourmaline: Description and crystal structure. American Mineralogist, 83, 896–900.
Selway, J.B., Novák, M., Černý, P., and Hawthorne, F.C. (1999) Compositional evolution of tourmaline in lepidolite-subtype pegmatites. European Journal of Mineralogy, 11, 569–584.
Selway, J.B., Černý, P., Hawthorne, F.C., and Novák, M. (2000) The Tanco pegmatite at Bernic Lake, Manitoba. XIV. Internal tourmaline. Canadian Mineralogist, 38, 877–891.
Selway, J.B., Smeds, S.-A., Černý, P., and Hawthorne, F.C. (2002) Compositional evolution of tourmaline in the petalite-subtype Nyköpingsgruvan pegmatites, Utö, Stockholm Archipelago, Sweden. GFF, 124, 93–102.
Sokolov, P.B., Gorskaya, M.G., Gordienko, V.V., Petrova, M.G., Kretser, Yu.L., and Frank-Kamenetskii, V.A. (1986) Olenite, Na$_{1-x}$Al$_3$Al$_6$B$_3$Si$_6$O$_{27}$(O,OH)$_4$—a new high-alumina mineral of the tourmaline group. Zapiski Vsesoyuznogo Mineralogicheskogo Obshchestva, 115, 119–123.
Wise, M.A. (2000) Geochemical evolution of tourmaline in the Black Mountain pegmatite, Maine. GeoCanada 2000, Program with Abstracts, 622–625. GeoCanada 2000, Calgary, Alberta.
Wright, S.E., Foley, J.A., and Hughes, J.M. (2000) Optimization of site-occupancies in minerals using quadratic programming. American Mineralogist, 85, 524–531.

MANUSCRIPT RECEIVED APRIL 25, 2004
MANUSCRIPT ACCEPTED AUGUST 6, 2004
MANUSCRIPT HANDLED BY DARBY DYAR